Chapter 1

Introduction

Nuclear spin relaxation rates can be used to characterise atomic self-diffusion in solids. Relaxation rates can be measured as functions of temperature and applied magnetic field strength and direction in order to determine, for example: the diffusion mechanism, the values of activation energies, and the concentrations of impurity atoms in the solid. Detailed theory of both the nuclear interactions and the atomic diffusion is required, however, to interpret the experimental results accurately. The relaxation rate theory used in the present work is that given by Abragam (1961) and Slichter (1990) in which the relaxation rates are derived from first order perturbation theory, exact in the high-field limit, and can be written as linear combinations of spectral density functions. The spectral density functions are the Fourier transforms of ensemble-averaged autocorrelation functions of the magnetic dipole interactions between pairs of nuclei. These functions are written in terms of displacement probabilities which describe the diffusion of the nuclei, and which are the basis of calculating nuclear spin relaxation rates for different diffusion models.

In three-dimensional systems much work has been done calculating relaxation rates due to solid-state diffusion, especially for that by the vacancy mechanism. The initial approximation to the spectral density functions of Bloembergen *et al.* (1948) was extended by Torrey (1953) to the case of isotropic diffusion using random walk theory. Eisenstadt and Redfield (1963) introduced the concept of an atom-vacancy encounter to calculate relaxation rates due to the vacancy diffusion mechanism in solids, and this model can be used to calculate relaxation rates accurate in the low defect-concentration limit. Relaxation rates due to solid state diffusion have since

been calculated for many systems and by a variety of techniques, including: Monte Carlo simulations of the atomic diffusion to determine the displacement probabilities (Wolf 1974; Wolf *et al.* 1977; Faux *et al.* 1986); lattice summations in the case of diffusion by the simple random walk in three dimensions (Wolf 1975), and by the mean field theory (Sankey and Fedders 1979; Barton and Sholl 1980); and approximations to the lattice summations for diffusion by the vacancy mechanism using the encounter model (MacGillivray and Sholl 1986). The high- and low-frequency limiting forms of nuclear spin relaxation rates were calculated for diffusion in one-, two- and three-dimensional systems by Sholl (1981a). The aim of this thesis is to calculate the spectral density functions, and hence the nuclear spin relaxation rates, for lattice diffusion in some two-dimensional systems and for the interstitialcy diffusion mechanism in three-dimensional systems.

1.1 Two-dimensional systems

There are many systems in which atomic diffusion is restricted to two dimensions; such as layered compounds, intercalates, and diffusion on surfaces. Many of these systems are of significant technological importance, especially some of the layered ionic solids (for example, Na^+ β-alumina) which have high ionic conductivities at only moderately elevated temperatures, well below their melting points. Nuclear spin relaxation rate experiments can be used to study the atomic diffusion in these systems, but realistic diffusion models and the appropriate NMR spectral density function theory are required to interpret the results accurately.

Previously, the spectral density functions due to two-dimensional diffusion had been calculated for continuum diffusion models, such as the work of Avogadro and Villa (1977), Neue (1988), and the more sophisticated continuum diffusion models of Korb *et al.* (1983, 1984, 1987a, b, 1990). In Chapter 2, the spectral density functions are calculated for lattice diffusion on the two-dimensional square lattice. The cases of like- and unlike-spin interactions are considered, with interactions between nuclei on a single or on separate planes possible. The present work is an extension of the continuum diffusion models to lattice diffusion by the simple random walk and the mean field theories of diffusion, and this is the first application of these theories to calculating the spectral density functions due to two-dimensional diffusion. The

results are compared with the results of the continuum diffusion models of Neue (for interactions between nuclei on separate planes) and Avogadro and Villa (for interactions between nuclei diffusing in a single plane), and also with the results of the often-used BPP approximation (Bloembergen *et al.* 1948). The BPP model assumes that the autocorrelation function of interactions between pairs of nuclei behaves as a decaying exponential function with time and is equivalent to assuming a complete decorrelation of the interactions when either one of the nuclei first jumps to a new lattice site. This approximation is commonly used to interpret experimental data because of the simple Lorenzian form of the resulting spectral density functions. In the present work it is demonstrated that the BPP model is a particularly poor approximation of the results for two-dimensional diffusion, being less accurate than in the case of three-dimensional lattice diffusion. Also given is a technique for applying the mean field square lattice results as an approximation to other two-dimensional lattices, such as the hexagonal and honeycomb structures, so that the approximation is exact in the high-frequency limit.

The longitudinal relaxation rates R_1 and $R_{1\rho}$ in the laboratory and rotating frames of reference, respectively, are calculated in Chapter 2 for the like-spin magnetic dipole interaction between nuclei diffusing on a square lattice. The results for the mean field and BPP models of diffusion are compared, and the anisotropy of the relaxation rates with orientation of the applied magnetic field is examined.

1.2 Diffusion and relaxation due to the interstitialcy mechanism

Atomic self-diffusion within crystalline solids is largely due to the presence of point defects in the solid. Two common mechanisms of atomic diffusion by point defects in solids are the vacancy and interstitialcy mechanisms. Atomic displacement probabilities due to the vacancy diffusion mechanism, and the resulting nuclear spin relaxation rates in the cubic lattices have been well studied: Monte Carlo simulations of the vacancy motion were used by Wolf (1974) and Wolf *et al.* (1977) to calculate relaxation rates due to diffusion on the b.c.c. and f.c.c. lattices; Sholl (1974,

1982) and MacGillivray and Sholl (1986) have calculated the relaxation rates using approximations to the atomic displacement probabilities based on random walk theory; and, more recently, accurate analytic expressions for the atomic displacement probabilities—which are exact in the low vacancy-concentration limit—have been calculated by Sholl (1992). Relaxation rates due to diffusion by the forward noncollinear interstitialcy mechanism in a fluorite lattice have been calculated using Monte Carlo simulations of the interstitial defect motion (Wolf *et al.* 1977; Figueroa *et al.* 1979). In general, though, the interstitialcy diffusion mechanism has not received as much attention as has the vacancy diffusion mechanism.

In Chapter 3, accurate expressions for the atomic displacement probability are derived for diffusion by the interstitialcy mechanism. These expressions, which are used to calculate spectral density functions, are written in terms of the atom jump probabilities due to the diffusion of a single interstitial defect. A simple matrix expression, in terms of lattice generating functions, is derived which provides a straightforward means of evaluating the atom jump probabilities. The technique used is similar to that of Sholl (1992) for the vacancy diffusion mechanism, but is significantly extended to incorporate the two-stage jumps of the interstitialcy diffusion mechanism.

In addition to the atomic displacement probabilities, the atom jump probabilities can be used to calculate the tracer correlation factor, f, which characterises spatial correlations of the atomic diffusion. The diffusion coefficient, D, can be written as $D = fD_{\mathrm{un}}$ where D_{un} is the diffusion coefficient for uncorrelated diffusion in the system (see for example LeClaire 1970; Kelly and Sholl 1987). Many calculations and simulations of the tracer correlation factor have been undertaken, for a wide range of systems (see for example Allnatt and Lidiard 1993 for a recent review). Experimental measurements of the tracer correlation factor can be compared with theoretical values to help identify the dominant diffusion mechanism present in a system.

For the vacancy mechanism of diffusion in some structures, analytic expressions for the atom jump probabilities are known in terms of the lattice generating functions (Szabó *et al.* 1991; Sholl 1992), and can be used to evaluate the tracer correlation factor. In the cubic lattices, the square lattice, and the diamond and honeycomb structures the tracer correlation factor for the vacancy diffusion mechanism is found

Table 1.1: Values of the tracer correlation factor, f, (given by equation (1.1)) and the expressions and values of A for diffusion by the vacancy mechanism in various structures, arranged in order of increasing coordination number, Z. The value of A for the square and hexagonal lattices are due to Montet (1973) and those for the honeycomb and diamond structures are due to Szabó *et al.* (1991).

	Z	A	f
Honeycomb	3	$P_0 - P_2 = \frac{Z}{Z-1}$	$1 - \frac{2}{Z} = \frac{1}{3}$
Square	4	$P_0 - P_3 = \frac{4(\pi-2)}{\pi}$	$\frac{1}{\pi-1} = 0.4669422$
Diamond	4	$P_0 - P_2 = \frac{Z}{Z-1}$	$1 - \frac{2}{Z} = \frac{1}{2}$
Hexagonal	6	$P_0 + P_1 - P_2 - P_3 = \frac{5\pi-6\sqrt{3}}{\pi}$	$\frac{\pi+6\sqrt{3}}{11\pi-6\sqrt{3}} = 0.5600570$
Simple-cubic	6	$P_0 - P_4 = 1.2590517$	0.6531088
Body-centred-cubic	8	$P_0 + P_2 - P_3 - P_5 = 1.2635794$	0.7271941
Face-centred-cubic	12	$P_0 + 2P_1 - 2P_3 - P_4 = 1.4721608$	0.7814514

to be of the form

$$f = 1 - \frac{2A}{Z + A} \tag{1.1}$$

where Z is the coordination number of the structure and A is a linear combination of lattice generating functions, P_j. The P_j are the mean number of times the vacancy, commencing its random walk from the origin, visits one of the j^{th} nearest neighbour sites. The method of calculating the P_j for Bravais and non-Bravais lattices is given in an appendix in the present work, and Table 1.1 shows the expressions and values of A and the values of f calculated by equation (1.1) for diffusion by the vacancy mechanism in various lattices.

In Chapter 3, the tracer correlation factor for diffusion by the interstitialcy mechanism is demonstrated to have a general form which has similarities to equation (1.1). The result is

$$f = 1 - \frac{AB^2}{\alpha(\alpha Z' - AB)} \tag{1.2}$$

where A and B are linear combinations of lattice generating functions and defect jump probabilities, respectively, and the α and Z' are geometric factors which depend on the lattice type. A special case is that of the collinear interstitialcy diffusion mechanism for which $A = 1$ and $B = \alpha$, and the expression (1.2) for the tracer correlation factor

simplifies to

$$f = 1 - \frac{1}{Z' - 1}. \tag{1.3}$$

This remarkably simple expression for f depends only on the number of possible jumps, Z', of an interstitial defect and is valid for all the interstitial systems considered in the present work.

In Chapter 4, the accurate expressions for the atomic displacement probabilities due to the vacancy and interstitialcy diffusion mechanisms in the NaCl structure are applied, for the first time, to nuclear spin relaxation rate theory. The encounter model of Eisenstadt and Redfield (1963), in which the diffusion proceeds by an uncorrelated sequence of atom-defect encounters, is used to describe the diffusion of the cations. The results, therefore, are exact only in the low defect-concentration limit where the mean time between encounters is much greater than the mean duration of an encounter. Simple analytic approximations to the spectral density functions for unlike-spin magnetic dipole interactions in the NaCl structure are found which provide a straightforward means of calculating nuclear spin relaxation rates.

The relaxation rates of F nuclei in solid LiF (which has the NaCl structure) due to magnetic dipole interaction with the Li nuclei diffusing by the vacancy and interstitialcy mechanisms are then calculated. One of the aims in doing so is to determine whether or not nuclear spin relaxation rate measurements can be used to determine the dominant diffusion mechanism present in LiF. Relaxation rates for diffusion in polycrystalline samples and single crystals at various orientations are found and compared with the corresponding results of the BPP approximation. The low-frequency results are also studied by considering the relaxation rate differences $R_2 - R_{1\rho}$ and $R_{1\rho} - R_1$, which highlight some of the shortcomings of the BPP approximation.

Conclusions to each section of the present work are given at the end of the appropriate chapters, commencing on pages 30, 57 and 81.

Some aspects of the work presented here have been published in the papers listed at the end of the thesis.

Chapter 2

NMR magnetic dipolar spectral density functions for two-dimensional lattice diffusion

2.1 Introduction

The theory of nuclear spin relaxation due to fluctuating magnetic dipolar interactions involves, in the weak collision limit, spectral density functions which depend on the nature of the fluctuations. If the time dependence of the dipolar interactions is due to translational diffusion of the spins it is well known that the functional form of the spectral density functions depends on the dimensionality of the system (see for example Sholl 1981a), especially in the rapid diffusion limit corresponding to high temperatures or low resonant frequencies. In the case of interacting spins undergoing two-dimensional diffusion in a plane the spectral density functions depend on the frequency ω according to $\log(1/\omega)$ in the low frequency limit under very general conditions.

The evaluation of the spectral density functions for two-dimensional systems has been considered for continuum diffusion models by Avogadro and Villa (1977) and Korb *et al.* (1983, 1984, 1987a) for the case where the dipolar interactions are all in a plane. The extension of this theory to the diffusing spins in a plane interacting with spins in a separate parallel plane has been treated by Korb *et al.* (1987b) and

Neue (1988). The continuum diffusion models are appropriate for systems in which the mobile spins behave like two-dimensional liquids but may not be good approximations for spins undergoing diffusion on a lattice. The high-frequency form of the spectral density functions for spins diffusing on a square and hexagonal lattices has been derived by MacGillivray and Sholl (1985a, b) but there are no results available for discrete lattice diffusion over the entire frequency range.

The aim of the present chapter is to calculate the spectral density functions and nuclear spin relaxation rates over the complete frequency range for some lattice diffusion models and to compare the results to those for continuum diffusion models and the BPP model (Bloembergen *et al.* 1948). The general theory is developed for arbitrary two-dimensional structures and is applied specifically to the case of a square lattice. The cases of spins interacting with each other in the same plane and of spins in one plane interacting with spins in a separate parallel plane are both considered. The form of the dependence of the spectral density functions and relaxation rates on the direction of the applied magnetic field relative to the crystal axes is more involved for the square lattice than for the continuum model and results for this angular dependence are presented.

2.2 Spectral density functions

The spectral density functions relevant to nuclear spin relaxation due to magnetic dipolar interactions, for both like and unlike spin interactions, are (Abragam 1961; Sholl 1981a)

$$J^{(p)}(\omega) = cd_p^2 \sum_{\alpha,\beta} \frac{Y_{2p}^*(\Omega'_\alpha)}{r_\alpha^3} \frac{Y_{2p}(\Omega'_\beta)}{r_\beta^3} P(\mathbf{r}_\alpha, \mathbf{r}_\beta, \omega) \tag{2.1}$$

where $d_0^2 = 16\pi/5$, $d_1^2 = 8\pi/15$, $d_2^2 = 32\pi/15$, $Y_{2p}(\Omega')$ are spherical harmonics normalised to unity, $\mathbf{r}_\alpha = (r_\alpha, \Omega'_\alpha)$ are vectors separating the interacting spins, and c is the probability of finding a spin at $\mathbf{r}_\alpha$ relative to one at the origin. The function $P(\mathbf{r}_\alpha, \mathbf{r}_\beta, \omega)$ is the Fourier transform

$$P(\mathbf{r}_\alpha, \mathbf{r}_\beta, \omega) = 2 \int_0^\infty P(\mathbf{r}_\alpha, \mathbf{r}_\beta, t) \cos \omega t \, dt \tag{2.2}$$

of $P(\mathbf{r}_\alpha, \mathbf{r}_\beta, t)$ which is the probability of a pair of spins being separated by $\mathbf{r}_\beta$ a time t after they were separated by $\mathbf{r}_\alpha$. The directions Ω'_α of the spherical harmonics are

relative to the direction of the applied magnetic field.

The dependence of $J^{(p)}(\omega)$ on the orientation of the crystal with respect to the magnetic field direction can be expressed in terms of trigonometric functions of the polar angles (θ, ϕ) of the field direction relative to crystal axes and functions $J_{pp'}(\omega)$ defined for p and $p' = -2$ to 2, by (Sholl 1986)

$$J_{pp'}(\omega) = c \sum_{\alpha,\beta} \frac{Y^*_{2p}(\Omega_\alpha)}{r^3_\alpha} \frac{Y_{2p'}(\Omega_\beta)}{r^3_\beta} P(\mathbf{r}_\alpha, \mathbf{r}_\beta, \omega) \tag{2.3}$$

where the directions of the spherical harmonics are now relative to axes fixed in the crystal. The z direction will be chosen to be the normal to the plane of the diffusing spins.

The maximum number of independent nonzero parameters needed to specify $J^{(p)}(\omega)$ for each frequency is 15 and crystal symmetry reduces this number (Sholl 1986). If the z axis is a 6-fold rotation axis or if there is circular symmetry about the z axis, as is the case for a continuum diffusion model, only the three (real) diagonal elements of $J_{pp'}(\omega)$ are nonzero and $J^{(p)}(\omega)$ depends only on θ according to

$$d_p^{-2} J^{(p)}(\omega) = J_{pp} + B_p \sin^2\theta + C_p \sin^4\theta, \tag{2.4}$$

where

$$B_0 = 3(J_{11} - J_{00}), \quad B_1 = \frac{1}{2}(3J_{00} - 5J_{11} + 2J_{22}), \quad B_2 = J_{11} - J_{22},$$

$$C_0 = \frac{3}{4}(3J_{00} - 4J_{11} + J_{22}), \quad C_1 = -\frac{2}{3}C_0, \quad C_2 = \frac{1}{6}C_0.$$

If the z axis is a 3- or 4-fold rotation axis $J^{(p)}(\omega)$ also depends on ϕ and there are additional terms to equation (2.4) given by

$$3D_p \sin^3\theta \cos\theta \, \Re(e^{3i\phi} J^*_{-12}) \qquad \text{3-fold axis} \tag{2.5}$$

$$\frac{3}{4} D_p \sin^4\theta \, \Re(e^{4i\phi} J^*_{-22}) \qquad \text{4-fold axis} \tag{2.6}$$

where $D_0 = 1$, $D_1 = -\frac{2}{3}$ and $D_2 = \frac{1}{6}$.

The number of independent (real) parameters is therefore 3 for a 6-fold rotation axis or circular symmetry, and 5 for a 3- or 4-fold rotation axis. If the dipolar interactions are restricted to the plane of diffusion, J_{11} and J_{-12} are zero because the spherical harmonics in equation (2.3) become zero. There are then only two

parameters (J_{00}, J_{22}) for a 3- or 6-fold rotation axes and 4 parameters (J_{00}, J_{22}, complex J_{-22}) for a 4-fold rotation axis. These results for the continuum diffusion in a plane are consistent with the angular expressions of Avogadro and Villa (1977) and the results for a 4-fold axis are consistent with the case $\phi = 0$ considered by MacGillivray and Sholl (1985a). (In equation (3.7) in the latter paper $f_2^{(0)}(\theta)$ should be $\frac{9}{4}\sin^4\theta$.)

The spherical average over all magnetic field directions $\langle J^{(p)}(\omega)\rangle$ of the spectral density functions in all cases is

$$\langle J^{(p)}(\omega)\rangle = \frac{d_p^2}{5}(J_{00} + 2J_{11} + 2J_{22}) \tag{2.7}$$

A circular average about the z axis gives the expression in equation (2.4) in all cases since the additional terms (2.5) and (2.6) average to zero.

Since the relaxation rates are linear combinations of the spectral density functions (Abragam 1961), the relaxation rates have the same functional form as $J^{(p)}(\omega)$ for their orientation dependence on the magnetic field direction and this is also the case for the appropriate averages over magnetic field directions.

In the weak-collision limit the experimentally measurable relaxation rates can be written as linear combinations of the spectral density functions $J^{(p)}(\omega)$. For example, for like-spin dipolar interactions the longitudinal relaxation rates R_1 and $R_{1\rho}$ in the laboratory and rotating frames, respectively, are (see for example, Kelly and Sholl 1992)

$$R_1 = 4C\left[J^{(1)}(\omega_0) + J^{(2)}(2\omega_0)\right] \tag{2.8}$$

$$R_{1\rho} = C\left[J^{(0)}(2\omega_1) + 10J^{(1)}(\omega_0) + J^{(2)}(2\omega_0)\right] \tag{2.9}$$

where $C = \frac{3}{8}\gamma^4\hbar^2 I(I+1)\left(\frac{\mu_0}{4\pi}\right)^2$, γ is the gyromagnetic ratio of the nuclear spin with spin quantum number I, and ω_0 and ω_1 are the Larmor frequencies of the spins in the applied static and oscillating magnetic fields respectively. The spectral density functions $J^{(p)}(\omega)$ are expressed in terms of $J_{pp'}(\omega)$ by equations (2.4) to (2.6) and the $J_{pp'}(\omega)$ are defined relative to the crystal axes by equation (2.3).

It is convenient to discuss and present the results in terms of the dimensionless function $h_{pp'}(\omega\tau)$ which is related to $J_{pp'}(\omega)$ by

$$J_{pp'}(\omega) = \frac{c\tau}{a^6} S_{pp'}\, h_{pp'}(\omega\tau) \tag{2.10}$$

where τ is a characteristic correlation time of the diffusion which is discussed in §2.3, $S_{pp'}$ is the lattice summation

$$S_{pp'} = a^6 \sum_{\alpha} \frac{Y^*_{2p}(\Omega_\alpha) Y_{2p'}(\Omega_\alpha)}{r^6_\alpha}, \tag{2.11}$$

and a is the lattice parameter, or the mean jump distance. The values of $S_{pp'}$ depend only on the geometry of the spin system and values are given in §2.4.

2.3 Diffusion models

The systems to be considered are spins diffusing on two-dimensional lattices by random jumps to vacant nearest-neighbour lattice sites. The dipolar interaction may be between like spins undergoing relative diffusion on the same lattice or between unlike spins where the dipolar interaction is between a diffusing spin in a plane and a lattice of fixed spins in the same or another parallel plane or planes. For unlike spin interactions the probability function $P(\mathbf{r}_\alpha, \mathbf{r}_\beta, t)$ will be of the form

$$P(\mathbf{r}_\alpha, \mathbf{r}_\beta, t) = P(\mathbf{r}_\alpha - \mathbf{r}_\beta, t) \tag{2.12}$$

if the fixed spins do not influence the diffusion of the moving spins. This is not the case for the relative diffusion of like spins on the same lattice since each of a pair of diffusing spins will then interfere with the diffusion of the other; even in the limit of low spin-concentration corresponding to just two spins on the lattice.

2.3.1 BPP model

The BPP model for the spectral density functions is based on an approximation for $P(\mathbf{r}_\alpha, \mathbf{r}_\beta, t)$ which corresponds to the pair of spins maintaining their relative separation for a mean time τ and assuming that the correlation in their dipolar interaction is completely destroyed when a jump of one of the spins occurs. It is therefore equivalent to choosing $P(\mathbf{r}_\alpha, \mathbf{r}_\beta, t)$ to be $\delta_{\alpha\beta} \exp(-t/\tau)$. The parameter τ is τ_c for the unlike-spin case where only one spin is mobile with a mean time of τ_c between jumps and is $\tau_c/2$ when either spin can jump, as in the like-spin case. The resulting dimensionless spectral density functions $h_{pp'}(\omega\tau)$ for the BPP model are zero if $S_{pp'} =$

0 and otherwise are

$$h_{pp'}(\omega\tau) = \frac{2}{1+(\omega\tau)^2} \tag{2.13}$$

which are independent of p, p', the crystal structure and any microscopic details of the diffusion process other than τ. These spectral density functions are simple to use and so this BPP model is widely used in analysing nuclear spin relaxation data, despite the approximations inherent in it.

2.3.2 Continuum model

In the limit of large distances and long times the lattice diffusion will be describable by the continuum diffusion expression in two-dimensions which is

$$P(\mathbf{r}_\alpha, \mathbf{r}_\beta, t) = \frac{1}{4\pi Dt} \exp\left\{\frac{-(\mathbf{r}_\alpha - \mathbf{r}_\beta)^2}{4Dt}\right\} \tag{2.14}$$

where the diffusion constant D is related to the lattice diffusion by $D = a^2/(4\tau_c)$, a^2 is the mean square jump length and τ_c is the mean time between jumps of a spin. This is the model considered by Neue (1988) for interactions between unlike spins where one of the two spin-types is fixed while the other diffuses on a second plane a distance z from the first. The resulting spectral density functions can be written in the form

$$J_{pp'}(\omega) = \delta_{pp'}\binom{4}{2-|p|}\frac{5n\tau}{6z^2a^2}C(\omega\tau_z) \tag{2.15}$$

$$C(u) = \int_0^\infty x^5\left(x^4 + \frac{9u^2}{4}\right)^{-1}\exp(-2x)\,dx \tag{2.16}$$

where n is the surface density of lattice sites and where τ_z is a parameter with the dimensions of time defined by

$$\tau_z = \frac{8z^2\tau}{3a^2}. \tag{2.17}$$

The parameter τ in these expressions is τ_c if only one spin is diffusing and becomes $\tau_c/2$ if both spins are diffusing. In the limit of large $\omega\tau_z$ ($\omega\tau z^2 \to \infty$), $C(\omega\tau_z) = 5/[6(\omega\tau_z)^2]$ so that

$$J_{pp'}(\omega) = \delta_{pp'}\binom{4}{2-|p|}\frac{25na^2\tau}{256}\frac{1}{z^6}\frac{1}{(\omega\tau)^2} \tag{2.18}$$

in this limit. For small values of $\omega\tau_z$ ($\omega\tau z^2 \ll 1$) the $J_{pp}(\omega)$ are linear in $\omega\tau$ and

$$J_{pp'}(\omega) \approx \delta_{pp'}\binom{4}{2-|p|}\frac{5n\tau}{6a^2}\left[\frac{1}{4z^2} - \frac{\pi}{a^2}\omega\tau\right]. \tag{2.19}$$

The expression (2.15) diverges as $z \to 0$ since the model then allows the unphysical condition that the two interacting spins can occupy the same site. An approximation for $z = 0$ which overcomes this difficulty is to limit the starting and finishing separations of the spins to regions outside circles of radius d. A similar analysis to Neue then gives (Avogadro and Villa 1977)

$$J_{pp'}(\omega) = \delta_{pp'} A_p \frac{4\tau n}{d^2 a^2} C_p(\omega \tau_D) \tag{2.20}$$

$$C_p(u) = \int_0^\infty x^5 (x^4 + u^2)^{-1} \left[\int_x^\infty \frac{J_{|p|}(y)}{y^2}\, dy \right]^2 dx \tag{2.21}$$

where $A_0 = 5/4$, $A_{\pm 1} = 0$, $A_{\pm 2} = 15/8$, $\tau_D = 4\tau d^2/a^2$ and the $J_{|p|}(y)$ are Bessel functions. The parameter τ is again τ_c for one spin diffusing and $\tau_c/2$ for both spins diffusing. More sophisticated continuum diffusion models have been considered by Korb *et al.* (1983, 1984, 1987a, b, 1990).

2.3.3 Random walk model

A general approach to evaluating the spectral density functions for discrete lattice diffusion is to use a reciprocal-space formalism (Fedders and Sankey 1978; Barton and Sholl 1980) in which

$$J_{pp'}(\omega) = \frac{A^2}{(2\pi)^4} \iint T_p^*(\boldsymbol{q}, \boldsymbol{j}, z) T_{p'}(\boldsymbol{q}', \boldsymbol{j}, z) P(\boldsymbol{q}, \boldsymbol{q}', \omega)\, d\boldsymbol{q}\, d\boldsymbol{q}' \tag{2.22}$$

where the integrals are over the first Brillouin zone of the two-dimensional reciprocal lattice (see Appendix A), A is the area of the two-dimensional unit cell, $P(\boldsymbol{q}, \boldsymbol{q}', \omega)$ is the temporal and spatial Fourier transform of $P(\mathbf{r}_\alpha, \mathbf{r}_\beta, t)$ and

$$T_p(\boldsymbol{q}, \boldsymbol{j}, z) = \sum_{\boldsymbol{l}} \frac{Y_{2p}(\Omega_\alpha)}{r_\alpha^3} \exp(i\boldsymbol{q} \cdot \mathbf{r}_\alpha) \tag{2.23}$$

where $\mathbf{r}_\alpha = \boldsymbol{l} + \boldsymbol{j} + z\hat{\boldsymbol{k}}$. The vectors $\boldsymbol{l}$ are two-dimensional lattice vectors (in the xy-plane) and $\boldsymbol{j} + z\hat{\boldsymbol{k}}$ is the relative displacement of a planar lattice of fixed spins from the planar lattice of diffusing spins, where z is the separation between the planes and $\boldsymbol{j}$ is a planar vector characterising the relative displacement of the lattices parallel to the planes. For like-spin dipolar interactions in a plane, $\boldsymbol{j}$ and z are both zero and the term $\boldsymbol{l} = 0$ must be omitted from the summation in the expression (2.23). An

efficient method of evaluating lattice summations of the form of $T_p(\boldsymbol{q},\boldsymbol{j},z)$ is to use the Poisson summation formula (Barton and Sholl 1980) and the resulting expressions for the two-dimensional summations are given in Appendix B.1. A particular lattice diffusion model will determine $P(\boldsymbol{q},\boldsymbol{q}',\omega)$ and $J_{pp'}(\omega)$ can then be evaluated using equation (2.22) and the expressions in Appendix B.1. The symmetry of the calculated $J_{pp'}(\omega)$ will be as discussed in §2.2.

A simple model of the diffusion of a spin is that it follows a random walk with a mean time of τ_c between jumps. Random walk theory (Barber and Ninham 1970) and equation (2.12) then give the expression

$$P(\boldsymbol{q},\boldsymbol{q}',\omega) = \frac{2\tau(2\pi)^2[1-\phi(\boldsymbol{q})]}{[1-\phi(\boldsymbol{q})]^2+(\omega\tau)^2}\delta(\boldsymbol{q}-\boldsymbol{q}'), \tag{2.24}$$

where $\tau = \tau_c$ for one spin diffusing and $\tau = \tau_c/2$ for both spins diffusing, $\phi(\boldsymbol{q})$ is the lattice structure factor, defined by

$$\phi(\boldsymbol{q}) = \sum_k w_k \exp(i\boldsymbol{q}\cdot\mathbf{r}_k) \tag{2.25}$$

and w_k is the probability that the jump of a spin from the origin will be to $\mathbf{r}_k$. For nearest neighbour jumps on a square lattice with lattice parameter a

$$\phi(\boldsymbol{q}) = \frac{1}{2}\big[\cos(q_1 a)+\cos(q_2 a)\big]. \tag{2.26}$$

In the limit of small $\omega\tau$, which corresponds to long range diffusion, and as $z\to\infty$ in such a way that $\omega\tau z^2 \to 0$, the spectral density functions of the random walk and the continuum models are equal. In these limits equation (2.19) for the continuum model of diffusion is also valid for the random walk model.

If a fraction, c, of the lattice sites are occupied by diffusing spins the mean time τ_c between jumps of a spin is $\tau_0/(1-c)$, where τ_0 is the mean time between jumps of a spin if it is the only spin on the lattice. For unlike spin dipolar interactions between fixed spins and diffusing spins the random walk model is exact in the limit $c\to 0$ and will be a reasonable approximation at other concentrations, except in the limit $c\to 1$ since the diffusion is then controlled by the random walks of vacancies. In three dimensions the encounter model (Wolf 1979a; MacGillivray and Sholl 1986; Sholl 1992) is then valid but this will not be applicable to two-dimensional systems. This is because an encounter cannot then be defined and Brummelhuis and Hilhorst (1988, 1989) have recently analysed the random walk theory for the limit of $c\to 1$ in two-dimensional systems.

2.3.4 Mean field model

The random walk model for like-spin dipolar interactions between two spins diffusing on the same lattice allows the unphysical possibility of the pair of spins both occupying the same site and therefore requires exclusion of the term $\boldsymbol{l} = 0$ in expression (2.23). It is therefore not rigorously correct even in the limit $c \rightarrow 0$. An improved theory, which will be referred to as the mean-field model, is to take into account the site-blocking effects of the two spins rigorously but to take the effects of the other spins into account only through the mean time τ_c between jumps as for the random walk model. This mean field model will again not be valid in the limit $c \rightarrow 1$ but is exact in the limit $c \rightarrow 0$. The results of a comparison between the random walk and mean field models for the spectral density functions in cubic crystals (Barton and Sholl 1980) suggested that the difference between the results for these models increases as the lattice coordination number decreases. It would therefore be expected that the difference between the $J^{(p)}(\omega)$ for the two models would be significant for planar systems, which can have low coordination numbers.

The evaluation of $P(\boldsymbol{q}, \boldsymbol{q}', \omega)$ for the mean field model in two dimensions is similar to that in three dimensions (Barton and Sholl 1980). The rate equation for $P(\mathbf{r}_\alpha, \mathbf{r}_\beta, t)$ can be found by considering the possible nearest neighbour jumps and jump rates of the spins, and is

$$\frac{d}{dt}P(\mathbf{r}_\alpha, \mathbf{r}_\beta, t) = \frac{2}{\tau_c}\left\{\frac{1}{Z}\sum_{i=1}^{Z} P(\mathbf{r}_\alpha, \mathbf{r}_\beta + \boldsymbol{n}_i, t)\left[1 - \delta_{\mathbf{r}_\beta,0} - \sum_{j=1}^{Z}\delta_{\mathbf{r}_\beta,\boldsymbol{n}_j}\delta_{\boldsymbol{n}_i,-\boldsymbol{n}_j}\right]\right.$$
$$\left. - P(\mathbf{r}_\alpha, \mathbf{r}_\beta, t)\left[1 - \delta_{\mathbf{r}_\beta,0} - \frac{1}{Z}\sum_{j=1}^{Z}\delta_{\mathbf{r}_\beta,\boldsymbol{n}_j}\right]\right\}, \qquad (2.27)$$

with the initial condition $P(\mathbf{r}_\alpha, \mathbf{r}_\beta, 0) = \delta_{\mathbf{r}_\alpha,\mathbf{r}_\beta}(1 - \delta_{\mathbf{r}_\beta,0})$, and where the $\boldsymbol{n}_i$ are the Z nearest neighbour vectors of the lattice. The terms without delta functions in the rate equation are those corresponding to the analogous rate equation for a simple random walk, while the terms with delta functions are a result of accounting for the site-blocking effects of the mean field model. Fourier transforming the rate equation for $P(\mathbf{r}_\alpha, \mathbf{r}_\beta, t)$ gives the integral equation:

$$P_c(\boldsymbol{q}, \boldsymbol{q}', \omega) = 2d_0(\boldsymbol{q}', \omega)\left[(2\pi)^2\delta(\boldsymbol{q} - \boldsymbol{q}') - 1\right] + \frac{A}{(2\pi)^2}\int K(\boldsymbol{q}', \boldsymbol{q}_1)P_c(\boldsymbol{q}, \boldsymbol{q}_1, \omega)\, d\boldsymbol{q}_1, \qquad (2.28)$$

for $P_c(\boldsymbol{q},\boldsymbol{q}',\omega)$ where $d_0(\boldsymbol{q}',\omega)$ is as defined below, the integral is over the first Brillouin zone, A is the area of the unit cell, and where the kernel of the integral equation is

$$K(\boldsymbol{q}',\boldsymbol{q}_1) = \frac{2}{\tau_c} d_0(\boldsymbol{q}',\omega)\Big\{1 + \phi(\boldsymbol{q}_1 - \boldsymbol{q}') - \phi(\boldsymbol{q}_1) - \phi(\boldsymbol{q}')\Big\}. \tag{2.29}$$

The temporal Fourier transform of $P(\boldsymbol{q},\boldsymbol{q}',t)$ is defined to be

$$P_c(\boldsymbol{q},\boldsymbol{q}',\omega) = 2\int_0^\infty P(\boldsymbol{q},\boldsymbol{q}',t)\exp(i\omega t)\,dt \tag{2.30}$$

and the function $P(\boldsymbol{q},\boldsymbol{q}',\omega)$ required in the evaluation of the spectral density functions is the real part of $P_c(\boldsymbol{q},\boldsymbol{q}',\omega)$. It is assumed in the above definition that $P(\boldsymbol{q},\boldsymbol{q}',t)$ is an even function of t which is the convention used by Barton and Sholl (1980) following Abragam (1961).

The kernel of the above integral equation is degenerate and the solution can, therefore, be found by solving a system of algebraic equations. This involves a considerable amount of algebra, which is outlined in Appendix C for the square lattice, and in this case the solution is

$$P(\boldsymbol{q},\boldsymbol{q}',\omega) = \frac{2\tau(2\pi)^2[1-\phi(\boldsymbol{q})]}{[1-\phi(\boldsymbol{q})]^2 + (\omega\tau)^2}\delta(\boldsymbol{q}-\boldsymbol{q}') + \Re\left\{ d_0(\boldsymbol{q},\omega)d_0(\boldsymbol{q}',\omega)\sum_l \frac{F_l(\boldsymbol{q})F_l(\boldsymbol{q}')}{B_l(\omega)}\right\} \tag{2.31}$$

where

$$d_0(\boldsymbol{q},\omega) = \frac{\tau}{[1-\phi(\boldsymbol{q})] - i(\omega\tau)},$$

$$F_1(\boldsymbol{q}) = 2 - \cos(q_1 a) - \cos(q_2 a), \qquad F_2(\boldsymbol{q}) = \cos(q_1 a) - \cos(q_2 a),$$

$$B_1(\omega) = 2\tau - \frac{A}{(2\pi)^2}\int d_0(\boldsymbol{q},\omega)\Big\{2 - 4\cos(q_1 a) + \cos^2(q_1 a) + \cos(q_1 a)\cos(q_2 a)\Big\}\,d\boldsymbol{q},$$

$$B_2(\omega) = 2\tau - \frac{A}{(2\pi)^2}\int d_0(\boldsymbol{q},\omega)\Big\{\cos^2(q_1 a) - \cos(q_1 a)\cos(q_2 a)\Big\}\,d\boldsymbol{q},$$

where $\tau = \tau_c/2$ and the integrals in the above expressions for the $B_l(\omega)$ are over the first Brillouin zone of the two-dimensional reciprocal lattice. The solution also involves $F_l(\boldsymbol{q})$ additional to those shown above but which do not contribute to the spectral density functions as the integrals over the Brillouin zone vanish by symmetry. The spectral density functions for the mean field model are then obtained from equations (2.22) and (2.23).

2.4 Results

Some numerical results are presented below for the spectral density functions and relaxation rates for diffusion on a square lattice. The spectral density functions $J_{pp'}(\omega)$ are related to their dimensionless forms $h_{pp'}(\omega\tau)$ by equation (2.10) and the values of the lattice summations $S_{pp'}$ for square lattices are given in Table 2.1. For simplicity, the only cases to be considered are unlike-spin dipolar interactions between diffusing spins in one plane and fixed spins in a parallel plane, where the planes are separated by $z > 0$, and like-spin dipolar interactions between spins diffusing in the same plane. Other similar like- and unlike-spin examples—including systems for which $\boldsymbol{j}$, the relative displacement of the planes parallel to the planes, is nonzero—are easily calculated and show similar qualitative features but are not considered here.

Table 2.1: Values of the lattice summations $S_{pp'}$, defined by equation (2.11), for a square lattice and for $z = 0$, a and $10a$ where a is the lattice parameter.

	$z = 0$	$z = a$	$z = 10a$
S_{00}	0.4634	0.4132	2.344×10^{-5}
S_{11}	0	0.1015	1.562×10^{-5}
S_{22}	0.6951	0.03851	3.905×10^{-6}
S_{-22}	0.5286	0.01070	-3.722×10^{-10}

2.4.1 Separate planes

The nonzero independent spectral density functions for square lattices with $z > 0$ and $\boldsymbol{j} = 0$ are $h_{pp}(\omega\tau)$ for $p = 0, 1, 2$ and the real part of $h_{-22}(\omega\tau)$. These functions are shown in Figure 2.1 for $z = 10a$ for the BPP and random walk models. The random walk results for $h_{pp}(\omega\tau)$ are the same for $p = 0, 1, 2$ to within 0.04% for this value of z. All of the functions are proportional to $(\omega\tau)^{-2}$ for large $\omega\tau$ as a result of this limit depending only on the details of the probabilities of no jump or one jump of a spin occurring in a time t. The range of $\omega\tau$ over which this limit is valid, however, is very different for the BPP and random walk models and increases with increasing z for the random walk model. This result is a consequence of the assumption in the

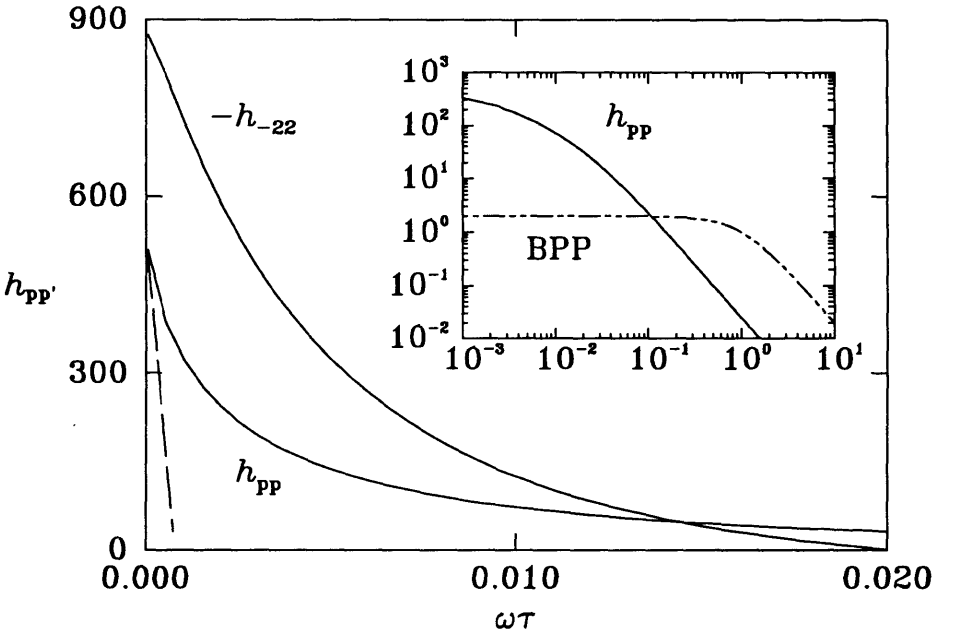

Figure 2.1: The functions $h_{pp'}(\omega\tau)$ for the random walk and BPP models for dipolar interactions between diffusing spins and fixed spins on square lattices separated by $z = 10a$. The BPP results are independent of p and p'. The broken line for small $\omega\tau$ shows the limiting linear form of $h_{pp}(\omega\tau)$ for the random walk model.

BPP model that the correlation in dipolar interactions is completely destroyed when a jump of a spin occurs. This becomes a poor approximation for large z because the jump of a spin then only involves a small change in the dipolar interaction between the spins while the random walk model includes the effect of this change correctly. The maxima in the relaxation rates occur at much smaller values of $\omega\tau$ for the random walk model than for the BPP model as z increases as a result of this difference between the models. The BPP model is also clearly a poor approximation, both in magnitude and in functional form, in the small $\omega\tau$ region and in the important range of $\omega\tau$ corresponding to the vicinity of the maxima in the relaxation rates.

The results for the continuum diffusion model are not shown in Figure 2.1 but agree with the random walk results to within 0.7% for $h_{pp}(\omega\tau)$ over the range of $\omega\tau$ shown. The function $h_{-22}(\omega\tau)$ is related to the angular dependence of the spectral density functions on the azimuthal angle ϕ, as discussed in §2.2, and it is zero for the continuum model but not for the random walk model.

The corresponding spectral density functions are shown for the case $z = a$ in

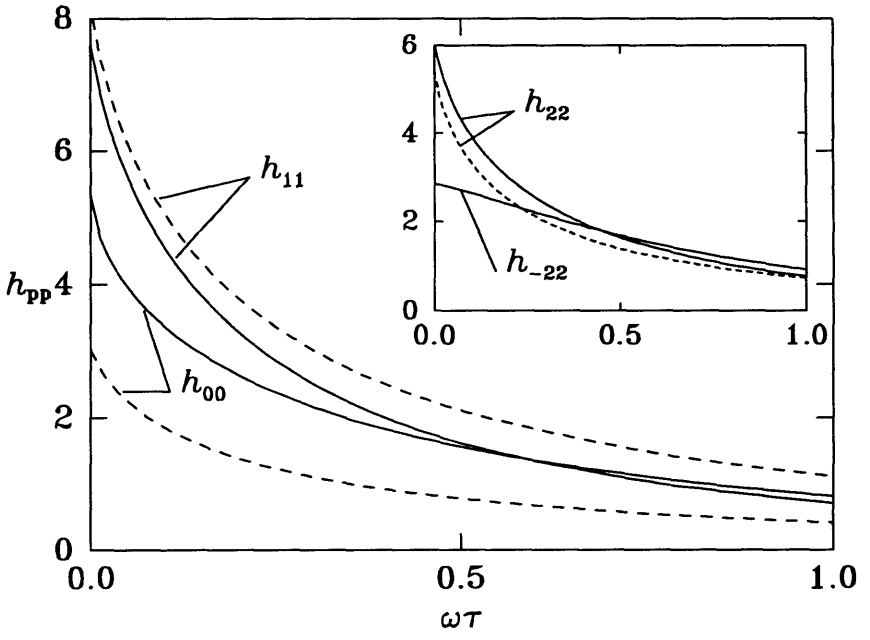

Figure 2.2: The functions $h_{pp'}(\omega\tau)$ for the random walk (——) and continuum (– – –) models for dipolar interactions between diffusing spins and fixed spins on square lattices separated by $z = a$. The function $h_{-22}(\omega\tau)$ is zero for the continuum model.

Figure 2.2 for the random walk and continuum models. The BPP results are not shown but are the same as in Figure 2.1 since they are independent of z. The magnitude of the BPP results are now comparable to the other models but the functional form is still quite different at small $\omega\tau$. The results for the random walk model show significant differences from those of the continuum model, unlike the case for $z = 10a$.

The general conclusions are therefore that the BPP model is unsatisfactory for these systems and that the continuum model is a good approximation for $h_{pp}(\omega\tau)$ for large z. This latter result is expected since the details of the lattice structure will become less important as z increases. Lattice diffusion models such as the random walk model are however necessary for small z and for calculating $h_{-22}(\omega\tau)$ since this is zero for a continuum model.

2.4.2 Single plane

For like-spin interactions between spins diffusing in the same plane ($z = 0$) the function $h_{11}(\omega\tau) = 0$ and the functions $h_{00}(\omega\tau)$, $h_{22}(\omega\tau)$ and $h_{-22}(\omega\tau)$ are shown in

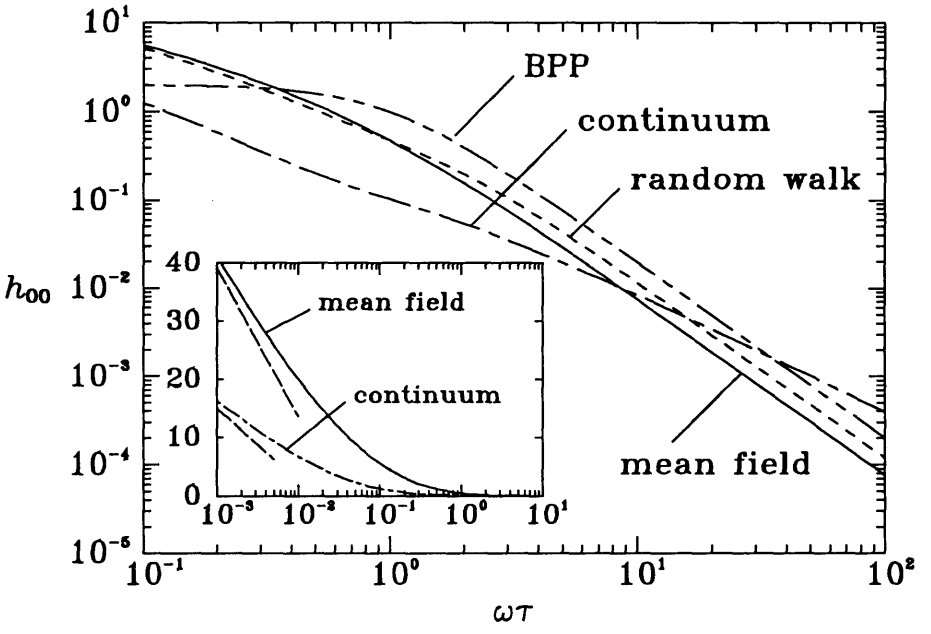

Figure 2.3: The function $h_{00}(\omega\tau)$ for the BPP, random walk, mean field and continuum models for interactions between spins diffusing on a square lattice ($z = 0$). The approach of the mean field and continuum models to the $\ln(1/\omega\tau)$ limit for small $\omega\tau$ is shown in the inset.

Figures 2.3 and 2.4 for the BPP, random walk, mean field and continuum models. The BPP model is again an unsatisfactory approximation, especially in the small $\omega\tau$ limit where it becomes constant. As shown in Figure 2.3, the other models show $\ln(1/\omega\tau)$ behaviour for $h_{00}(\omega\tau)$ in this limit; although their magnitudes can be significantly different from each other. The remaining independent $h_{pp'}(\omega\tau)$ do not diverge at $\omega\tau = 0$ but intersect the $\omega\tau = 0$ axis with finite slope as shown in Figure 2.4. In the case of $h_{22}(\omega\tau)$, which is linear in $\omega\tau$ in the low-frequency limit, this slope is nonzero for all but the BPP model. The slope of $h_{-22}(\omega\tau)$ at $\omega\tau = 0$ is zero.

These results show that the precise details of the diffusion model are quite important for $z = 0$ with the more rigorous mean field results showing appreciable differences to those for the random walk model and especially to those for the continuum model. The percentage difference between the spectral density functions for the random walk and mean field models becomes constant at both small and large $\omega\tau$. It is interesting to note that the numerical calculations are easier to compute to a given accuracy over a wide range of $\omega\tau$ for the more realistic mean field model than

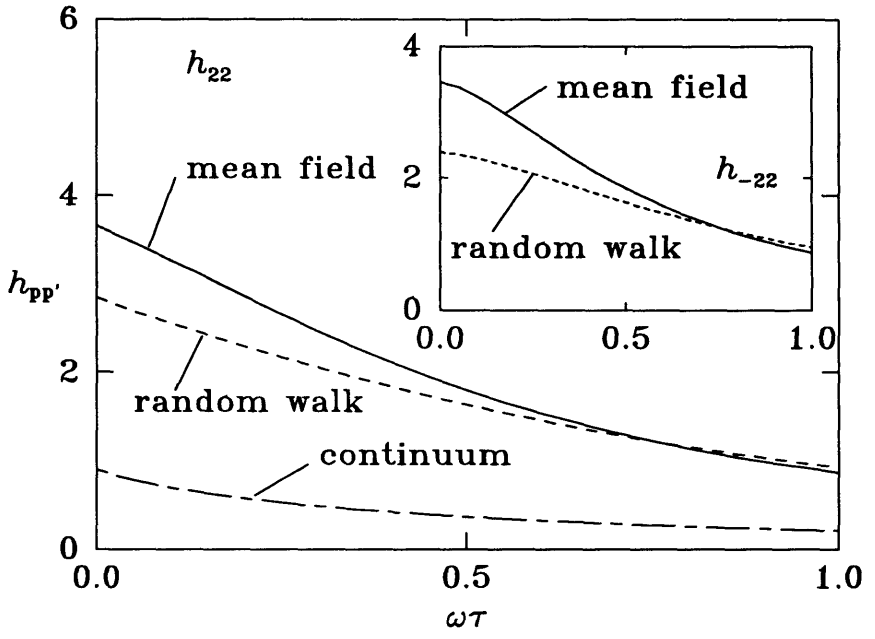

Figure 2.4: The functions $h_{22}(\omega\tau)$ and $h_{-22}(\omega\tau)$ for the same system as in Figure 2.3.

is the case for the continuum model.

Analytic approximations for the numerical results can be extremely useful (Sholl 1988) and the following functions have been found to fit the mean field results to good accuracy. The functions $h_{22}(\omega\tau)$ and $h_{-22}(\omega\tau)$ over the entire range of $\omega\tau$ and $h_{00}(\omega\tau)$ for $\omega\tau \geq 1.0$ may be approximated by

$$h_{pp'}(\omega\tau) = \frac{H}{a + b(\omega\tau) + c(\omega\tau)^u + d(\omega\tau)^v + (\omega\tau)^2} \tag{2.32}$$

where the values of the parameters and the accuracy of the approximations are given in Table 2.2.

A different functional form is required for $h_{00}(\omega\tau)$ for $\omega\tau < 1.0$ and the results can be described by

$$h_{00}(\omega\tau) = -\frac{11.150 \ln(29.81\omega\tau)}{[1 - 17.98(\omega\tau)^{0.87}]} \tag{2.33}$$

for $\omega\tau \leq 0.015$ accurate to within 0.6%. For $0.015 \leq \omega\tau \leq 2.5$

$$h_{00}(\omega\tau) = \frac{1}{\omega\tau} \sum_{n=0}^{5} \mathrm{A}_n x^n, \tag{2.34}$$

where $x = \log_{10}(2\omega\tau)$ and is also accurate to within 0.6% and where the coefficients A_n are

Table 2.2: Parameters for the analytic approximations to the mean field spectral density functions.

	$h_{00}(\omega\tau)$	$h_{22}(\omega\tau)$	$h_{-22}(\omega\tau)$
H	0.7577	1.3858	1.3377
a	0.25	0.3791	0.3869
b	0	0.3905	0
c	0.4028	−0.1879	0.4210
d	−0.0632	0.0268	−0.2783
u	0.80	1.50	1.11
v	1.40	1.80	1.30
maximum error	0.8%	1.1%	1.0%

$$\begin{aligned} A_0 &= 0.5995 & A_1 &= -0.2699 & A_2 &= -0.4929 \\ A_3 &= 0.0979 & A_4 &= 0.2289 & A_5 &= 0.0611. \end{aligned}$$

The low-frequency limit of $-11.150\ln(29.81\omega\tau)$ for the mean field model may be compared with $-5.395\ln(62.55\omega\tau)$ for the continuum model. The appreciable difference between these forms is shown in the inset of Figure 2.3. The low-frequency limits for the remaining independent spectral density functions for the mean field theory are $3.66 - (5\pi\omega\tau)/(2S_{22})$ for $h_{22}(\omega\tau)$ and 3.46 for $h_{-22}(\omega\tau)$.

As in the case of $z > 0$, the BPP model is again unsatisfactory in the present case of $z = 0$. The continuum diffusion model shows the correct functional form in the small-$\omega\tau$ limit but the magnitude is significantly in error, and again gives $h_{-22}(\omega\tau) = 0$. The lattice models are therefore necessary to give accurate results and also to give nonzero values of $h_{-22}(\omega\tau)$ and the mean field model is the most physically realistic of the models considered.

Application to diffusion on the hexagonal and honeycomb structures

Little, if any, experimental work has been done on systems with diffusion on a square lattice. There are, however, experimental results for diffusion on the two-dimensional hexagonal lattice (Heitjans 1993) and the honeycomb structure (Brinkman *et al.* 1982; Bader *et al.* 1992; Freiländer *et al.* 1987; Schirmer *et al.* 1992; McDowell *et al.* 1994). It is possible to apply the mean field theory to diffusion on these lattices, although

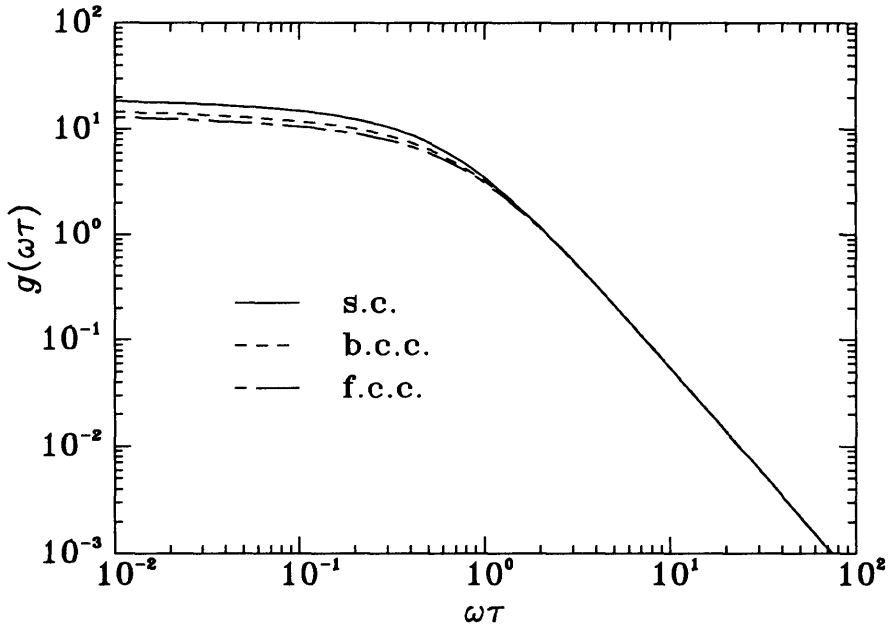

Figure 2.5: The spectral density functions, $g(\omega\tau) = \langle J^{(p)}(\omega)\rangle 4\pi a^6/(d_p^2\tau_c)$, for diffusion on the s.c., b.c.c. and f.c.c. lattices by the mean field model (Sholl 1988). The b.c.c. and f.c.c. curves are normalised to the s.c. curve in the high-frequency limit.

this has not been undertaken here. With little extra effort, however, the results for diffusion on a square lattice can be used to give reasonable first approximations to the cases of diffusion on the hexagonal lattice and honeycomb structure. It is straightforward to calculate the spectral density functions exactly in the high-frequency limit from rapidly converging lattice summations (Barton and Sholl 1980); the spectral density functions at lower frequencies then remain to be determined. The results for the three-dimensional diffusion on different lattice types indicate how a successful approximation to the spectral density functions at low frequencies might be found.

Figure 2.5 shows the spherical average of the spectral density functions of the mean field theory for three-dimensional diffusion on simple-cubic (s.c.), body-centred-cubic (b.c.c.) and face-centred-cubic (f.c.c.) lattices calculated by Sholl (1988). In this plot the b.c.c. and f.c.c. results have been normalised to the s.c. results in the high-frequency limit. It can be seen from the figure that the shape of the spectral density function curves for the mean field theory of three-dimensional diffusion is relatively insensitive to the lattice-type of the system for these lattices. The b.c.c. and f.c.c. results at low frequencies differ from the corresponding s.c. result by approximately

Table 2.3: Values of the dimensionless lattice summations, $S_{pp'}$, and the coefficients, H, of $(\omega\tau)^{-2}$ in the high-frequency limiting form of the dimensionless spectral density functions for diffusion on the hexagonal and honeycomb structures by the mean field theory. Also shown are scaling factors, k, for converting the results of diffusion on a square lattice to those of diffusion on the hexagonal and honeycomb structures.

	Hexagonal			Honeycomb		
	$S_{pp'}$	H	k	$S_{pp'}$	H	k
h_{00}	0.6342	0.6718	0.8867	0.3289	0.8249	1.0887
h_{22}	0.9513	1.7530	1.2650	0.4933	1.0905	0.7869
h_{-22}	-3.931×10^{-7}	1.9172	1.4332	-1.890×10^{-8}	1.3082	0.9779

21% and 30% respectively. The s.c. result, when scaled appropriately for the b.c.c. or f.c.c. systems, is therefore exact in the high-frequency limit and a reasonable order-of-magnitude approximation otherwise.

It is possible that a similar situation applies to the two-dimensional case; that is, the spectral density function results for the square lattice, when scaled to match the high-frequency limit of the hexagonal or honeycomb structure diffusion, could be a reasonable approximation at all other frequencies. For diffusion on the hexagonal and honeycomb structures the spectral density functions are proportional to $(\omega\tau)^{-2}$, as they are for the case of the square lattice, in the high-frequency limit. The values of the constant of proportionality, H, for each of the spectral density functions can be calculated from rapidly converging lattice summations (Barton and Sholl 1980), and the results of these calculations for the three independent $h_{pp'}(\omega\tau)$ for the mean field theory of diffusion on a single hexagonal lattice and on a single honeycomb structure are shown in Table 2.3. The parameter H is the parameter in the analytic approximation (equation (2.32)) of the spectral density functions for diffusion on the square lattice. Also shown in Table 2.3 are the dimensionless lattice summations, $S_{pp'}$, (equation (2.11)) and scaling factors, k, which when multiplied with the dimensionless spectral density functions for diffusion on the square lattice give the corresponding functions for diffusion on the hexagonal or honeycomb structures.

The spectral density functions for a square lattice, adjusted as described above

for a honeycomb structure, have been used to calculate the R_1 relaxation rate of hydrogen in $ZrBe_2H_{1.4}$ (McDowell *et al.* 1994) due to the like-spin magnetic dipole interaction between the H nuclei, where it is believed that the H nuclei diffuse on two-dimensional honeycomb structures. The resulting theoretical relaxation rate curves are shown fitted to the experimental data in Figure 2.6. It can be seen from this figure that the fit is particularly good at high temperatures. The theory self-consistently explains the positions of the maxima in addition to the frequency and temperature behaviour of the relaxation rates. The frequency dependence at high temperatures cannot be explained using the BPP approximation which is frequency independent in this region. Features of the relaxation rates due to the different diffusion models are discussed in the following section.

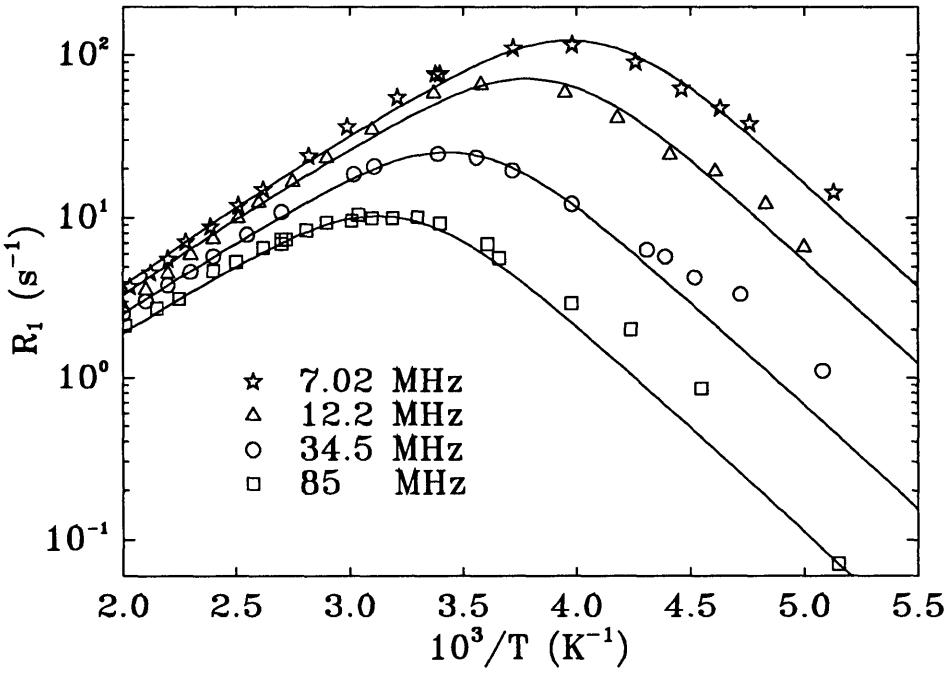

Figure 2.6: Experimental measurements of the R_1 relaxation rates in a powdered sample of $ZrBe_2H_{1.4}$, corrected for the conduction electron contribution. The curves are the spherically averaged relaxation rates for the mean field theory of diffusion on a square lattice, adjusted to approximate diffusion in the honeycomb structure. Data from McDowell *et al.* (1994).

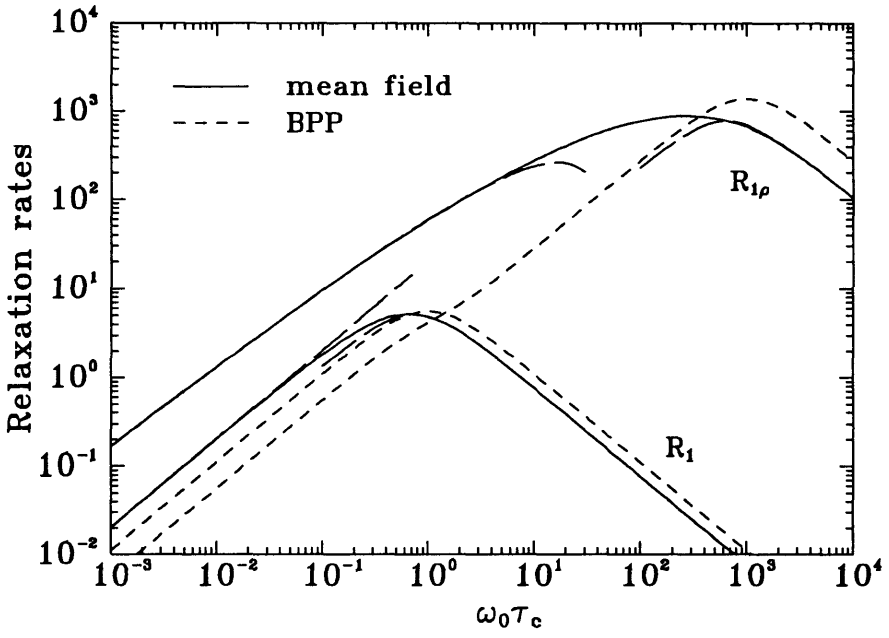

Figure 2.7: The relaxation rates R_1 and $R_{1\rho}$ as functions of $\omega_0\tau_c$ for interactions between spins diffusing on a square lattice. The results are for the magnetic field direction normal to the plane. The long-dashed lines correspond to the low-frequency limits in §2.4.2 and the high-frequency approximation of MacGillivray and Sholl (1985b).

2.4.3 Relaxation rates

The longitudinal relaxation rates R_1 and $R_{1\rho}$ are linear combinations of spectral density functions and are given by equations (2.8) and (2.9). The relaxation rates are dimensionless functions of $\omega_0\tau$ and $\omega_1\tau$ when expressed in units of $8\pi Cc/(15\omega_0 a^6)$ and plots of the relaxation rates in these units are shown in Figures 2.7 and 2.8 for the BPP and mean field models and various magnetic field orientations for like-spin interactions between spins diffusing on a square lattice ($z = 0$, $\boldsymbol{j} = 0$, $\tau = \tau_c/2$) and for $\omega_1 = \omega_0/10^3$. If the mean time, τ_c, between jumps depended on the temperature T according to an Arrhenius relation the relaxation rates plotted as functions of $\log(\omega\tau_c)$ would correspond to experimental relaxation rates plotted as functions of $1/T$.

Figure 2.7 shows the results for the BPP and mean field theories for the magnetic field direction oriented normal to the plane of spins. The form of the relaxation rates at large $\omega\tau$ (corresponding to high frequencies or low temperatures) is proportional to $(\omega\tau)^{-1}$ but there is a difference in magnitude between the models of 1.4 for R_1 and 2.6 for $R_{1\rho}$ in this limit. In the low-frequency (high-temperature) limit the BPP

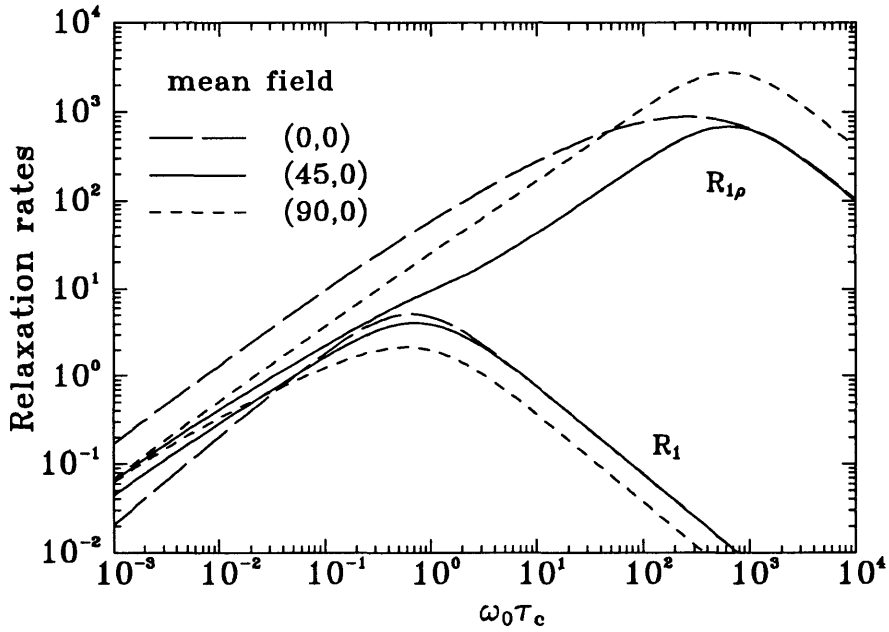

Figure 2.8: The mean field model results for some different magnetic field directions to those on Figure 2.7.

results are proportional to $\omega\tau$ for all magnetic field orientations, but this is true of the mean field model only for R_1, and then only if the magnetic field is normal to the plane of the spins, as in Figure 2.7. This is because, in this case, R_1 depends only on $h_{\pm 22}(\omega\tau)$ which do not show logarithmic behaviour for small $\omega\tau$. In all other cases the relaxation rates are not proportional to $\omega\tau$ for small $\omega\tau$ because the relaxation rates then depend on $h_{00}(\omega\tau)$ which shows logarithmic behaviour in this limit.

The relaxation rates for the mean field theory are shown in Figure 2.8 for three different orientations of the magnetic field direction. There are significant differences between the results for different field directions at all values of $\omega_0\tau_c$. The minimum and maximum values of the R_1 maximum for any field direction are 2.17 (in units of $8\pi Cc/(15\omega_0 a^6)$) at $\theta = 90°$, $\phi = 0°$ and 5.16 at $\theta = 0°$ respectively. The corresponding results for $R_{1\rho}$ are 123 at $\theta = 50°$, $\phi = 45°$ and 2770 at $\theta = 90°$, $\phi = 0°$.

The values of $\omega_0\tau_c$ and $\omega_1\tau_c$ at which the R_1 and $R_{1\rho}$ maxima occur are especially important parameters since they can provide directly a value of τ_c at the temperature for which the maximum relaxation rate occurs. The values of $\omega_0\tau_c$ for which the R_1 maxima occur are given as a function of magnetic field orientation for the BPP and

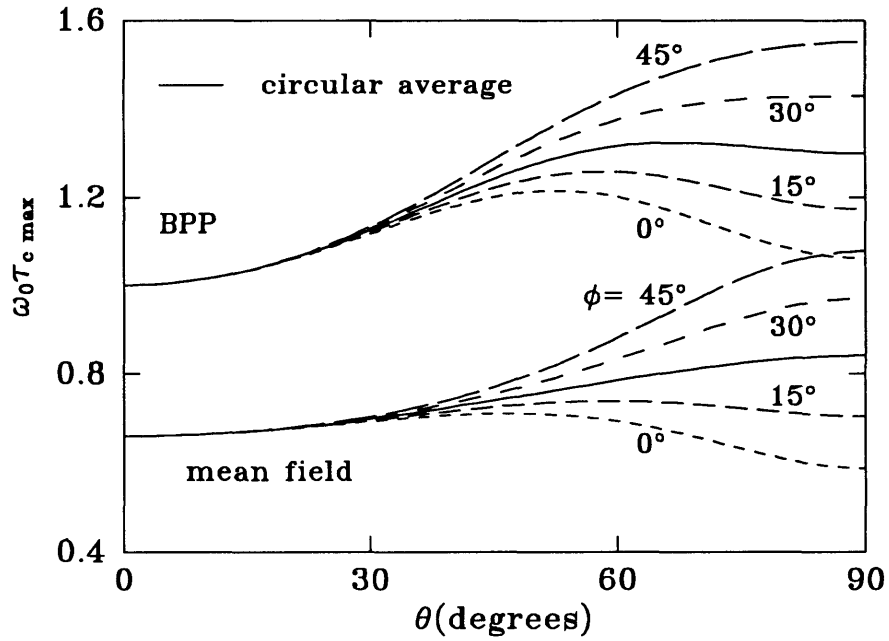

Figure 2.9: The values of $\omega_0\tau_c$ at which the maxima of R_1 occur as functions of the angles θ, ϕ of the magnetic field direction relative to the crystal axis.

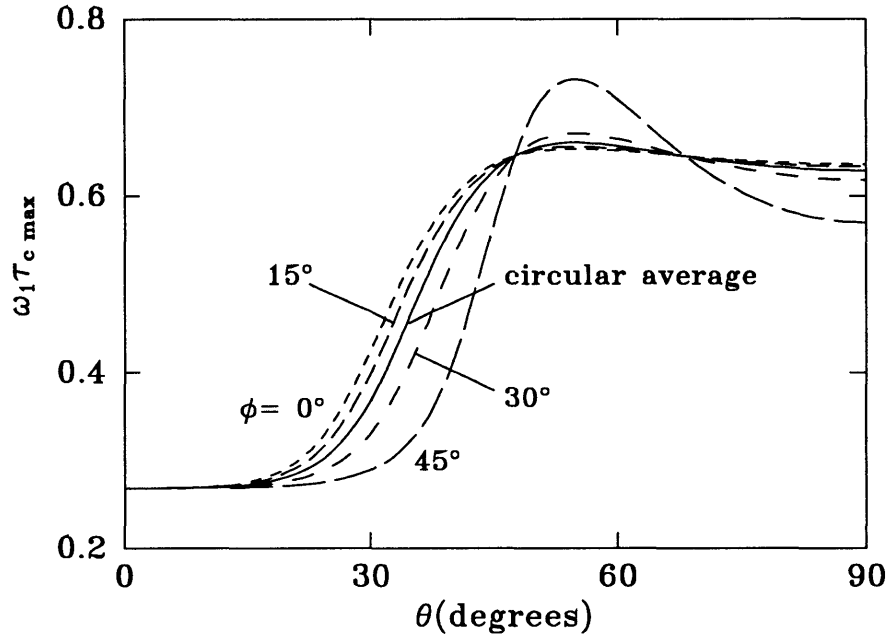

Figure 2.10: The values of $\omega_1\tau_c$ at which the maxima of $R_{1\rho}$ occur as functions of the magnetic field direction.

mean field theories in Figure 2.9 for the range of angles sufficient to specify the results for any orientation. It can be seen that the variation with θ, ϕ is similar for the two models but that the magnitudes are different. The comparable results for the mean field theory are given in Figure 2.10 for the $R_{1\rho}$ maximum. The corresponding BPP results are not shown but vary by only 0.02% over the entire range of θ and ϕ and the value is 1.0. Also shown in Figures 2.9 and 2.10 are the results for a circular average about the direction normal to the plane. The anisotropy of the position of the maxima is therefore quite different between the models for $R_{1\rho}$ compared with R_1. These results again show the inadequacy of the BPP model for two-dimensional systems.

Validity of field averaging the relaxation rates

The relaxation rates for polycrystalline samples can be obtained by taking the average, over all field directions, of the relaxation rates for a single crystal. As pointed out by Wolf (1975), however, it is the magnetisation rather than the relaxation rate that should be averaged. This leads to a non-exponential decay (or growth) of the magnetisation in a polycrystal, and Barton and Sholl (1976) have examined the validity of the approximation involved in averaging the relaxation rates for the simple random walk model in the (three-dimensional) cubic lattices. The approximation was found to be accurate for $\omega_0\tau_c \lesssim 2$ for both the R_1 and $R_{1\rho}$ relaxation rates. At high frequencies the deviation from the exponential decay becomes marked, especially in the case of the simple-cubic (s.c.) lattice for which the magnetisation has deviated 10% from the exponential approximation after times of $3.5\langle R_1\rangle$ and $0.95\langle R_{1\rho}\rangle$ for the R_1 and $R_{1\rho}$ relaxation respectively, and the approximation is worse for longer times. The times taken for the non-exponential decay of the magnetisation to deviate 10% from the exponential approximation as a function of $\omega_0\tau_c$ are shown in Figure 2.11.

Also shown in Figure 2.11 are the results of similar calculations for the mean field diffusion model in the two-dimensional square lattice. In this case the magnetisation has deviated from the exponential approximation by 10% after a time of $2.2\langle R_1\rangle$ for the R_1 relaxation at all frequencies except in the range $0.004 \lesssim \omega_0\tau_c \lesssim 0.2$ where the approximation is more accurate. The corresponding deviation for the $R_{1\rho}$ relaxation

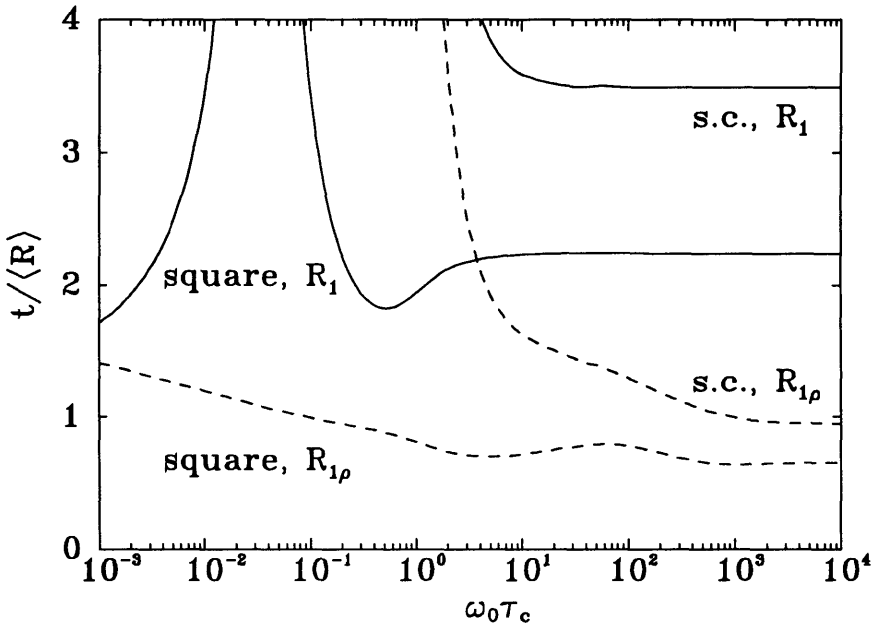

Figure 2.11: The time (in units of $\langle R \rangle$, the spherically averaged relaxation rate) taken for the non-exponential magnetisation decay to deviate 10% from the exponential approximation. The results are for the R_1 and $R_{1\rho}$ relaxation rates for random walk diffusion in a simple-cubic lattice, and the mean field model of diffusion in a square lattice.

occurs after a time of $0.65\langle R_{1\rho} \rangle$ for $\omega_1 \tau_c \gtrsim 1$, and after times ranging from approximately $\langle R_{1\rho} \rangle$ to $1.6\langle R_{1\rho} \rangle$ for $\omega_0 \tau_c \lesssim 1$. The assumption of an exponential decay of the magnetisation for a polycrystal is, therefore, a much poorer approximation in the case of two-dimensional diffusion than for three-dimensional diffusion, and it is likely that the non-exponential decay for a polycrystal with two-dimensional diffusion could be observed experimentally.

2.5 Conclusion

The functional form of the dependence of the spectral density functions as a function of the orientation of the magnetic field direction relative to the crystal axes has been obtained for dipole interactions between spins undergoing discrete lattice diffusion on separate parallel planes and for interactions between spins diffusing in a plane. The details of the reciprocal-space formulation for evaluating the spectral density

functions for two-dimensional lattice diffusion have been developed and applied to the random walk and mean field models for diffusion on a square lattice.

The results from the random walk and mean field models have been compared with the results from the BPP and continuum models. The BPP model is quite unsuitable for two-dimensional diffusion since it gives the incorrect functional form for the relaxation rates in the low-frequency (high-temperature) limit and can also give significant differences in the magnitudes of the spectral density functions and relaxation rates from the more detailed lattice diffusion models. The continuum model is quite satisfactory, as would be expected physically, for interactions between well separated planes but is less accurate for interactions between spins diffusing in a single plane. The lattice diffusion models are also necessary to calculate the dependence of the spectral density functions on the azimuthal angle between the magnetic field direction and the normal to the plane.

In the case of interactions in a single plane, the mean field model is exact in the limit of low spin concentrations and an accurate analytic approximation has been obtained for the spectral density functions for diffusion on a square lattice. These results should also be a good approximation for other spin concentrations which are not too large. The mean field model is a reasonable approximation for three-dimensional systems unless the spin concentration approaches unity (Faux *et al.* 1986). The range of spin concentrations over which the mean field model is valid might however be less for two-dimensional diffusion since the three-dimensional encounter model for high spin concentrations is not valid for two-dimensional diffusion.

While the functional form of the spectral density functions and relaxation rates in the high-frequency limit is similar for lattice diffusion models in one, two or three dimensions, this is not the case for the low-frequency limit. For example, anisotropic diffusion models in three-dimensional hexagonal crystals (Sholl 1987) showed significant differences between the results for one-, two- and three-dimensional diffusion. The spectral density functions for interactions in a plane show the $\ln(1/\omega\tau)$ behaviour as $\omega\tau \rightarrow 0$ but this limit is only approached for values of $\omega\tau$ corresponding to relaxation rates well below the maximum rate and might therefore be difficult to observe experimentally.

The relaxation rates for two-dimensional diffusion show a much stronger dependence on magnetic field direction than is the case for three-dimensional cubic systems.

An interesting consequence of this dependence on magnetic field direction is that the magnetisation recoveries show non-exponential behaviour at long times for polycrystalline samples (Barton and Sholl 1976). The stronger dependence on the field direction in two-dimensional systems means that the non-exponential magnetisation recoveries would be observed at shorter times.

The general analysis of two-dimensional systems developed above can be easily extended to other lattices and other like- and unlike-spin planar systems.